

**ICSO 2016**

**International Conference on Space Optics**

Biarritz, France

18–21 October 2016

*Edited by Bruno Cugny, Nikos Karafolas and Zoran Sodnik*



***Active support with set-and-forget characteristics for reflective optics***

*C. Reinlein*

*A. Brady*

*C. Damm*

*M. Mohaupt*

*et al.*



icso proceedings



International Conference on Space Optics — ICSO 2016, edited by Bruno Cugny, Nikos Karafolas,  
Zoran Sodnik, Proc. of SPIE Vol. 10562, 1056232 · © 2016 ESA and CNES  
CCC code: 0277-786X/17/\$18 · doi: 10.1117/12.2296192

**ACTIVE SUPPORT WITH ‘SET-AND-FORGET’ CHARACTERISTICS FOR REFLECTIVE OPTICS**

C. Reinlein<sup>1</sup>, A. Brady<sup>1</sup>, C. Damm<sup>1</sup>, M. Mohaupt<sup>1</sup>, A. Kamm<sup>1</sup>, M. Goy<sup>1,2</sup>.(Times New Roman, 10pt., centered)  
<sup>1</sup>Fraunhofer Institute for Applied Optics and Precision Engineering IOF, Albert-Einstein-Str.7, 07745, Jena, Germany. <sup>2</sup>Institute of Applied Physics, Abbe Center of Photonics, Friedrich Schiller University Jena, Max-Wien-Platz 1, 07743 Jena, Germany)

**INTRODUCTION**

An active support for large reflective optics is suitable to compensate for manufacturing-induced deformations and (re-)positioning-induced deformations such as induced by slewing of earth-based telescopes. In those applications, the control speed requirements are low as typical correction frequencies are around one Hertz. We believe that the complexity in Earth-based telescopes increases thanks to the application of more scientific instruments that are applied at cryogenic temperatures. Here temperature-induced deformations in reflective elements are likely to occur. In the standard procedure, the instrument is manufactured and then cooled to detect its optical surface quality. In the very likely case of temperature-induced aberrations, the instrument has to be de-assembled, the surfaces of the optics have to be re-machined before the instrument is assembled and tested again. This procedure is to repeat until the limitation of aberrations to a minimum/sufficient value. An application of active optics with a sufficient degree-of-freedom may compensate for cryogenic instrument aberrations if it is placed before the instrument. This would be beneficial as the active optics would not need to be cryo-compatible and could be considered as a part of the instrument if applied e.g., as a folding mirror. However, we believe that in this case each instrument would need such a mirror. In this case, a simple and reliable set-up is mandatory as the optimization of the wavefront is made once followed by a preferably long period without manipulation. Here we assume that the instrument characteristics are constant assuming a constant temperature. Further, the need of an active optics for each cryogenic instrument would also be a chance for to have a considerable number of required instruments that should be available with a reasonable price.

In space borne application active optics are also likely to be implemented to compensate for telescope aberrations. That aberrations may be caused by misalignment during unfolding after launch, gravity released aberrations in the optics, temperature-induced aberrations thanks to orbiting or misalignment of the optics due to telescope slewing. Beside orbiting- and slewing-induced aberrations are those aberrations static. And applications in L2 almost exclude these sources. Thus, we believe that space borne applications may further decrease the control loop frequency requirements, and the implementation of ‘set-and-forget’ actuation is consequentially. A set-and-forget actuation enables the optimization of the optical surface on-site followed by period without active manipulation.

The paper will remember the actuation mechanism as introduced earlier and will present extended results of the long-term stability. Moreover, we will present results of the best surface quality of the mirror and the fitting accuracy of typical Zernike polynomials.

**ACTIVE OPTICS MECHANISM AND CHARACTERIZATION RESULTS**

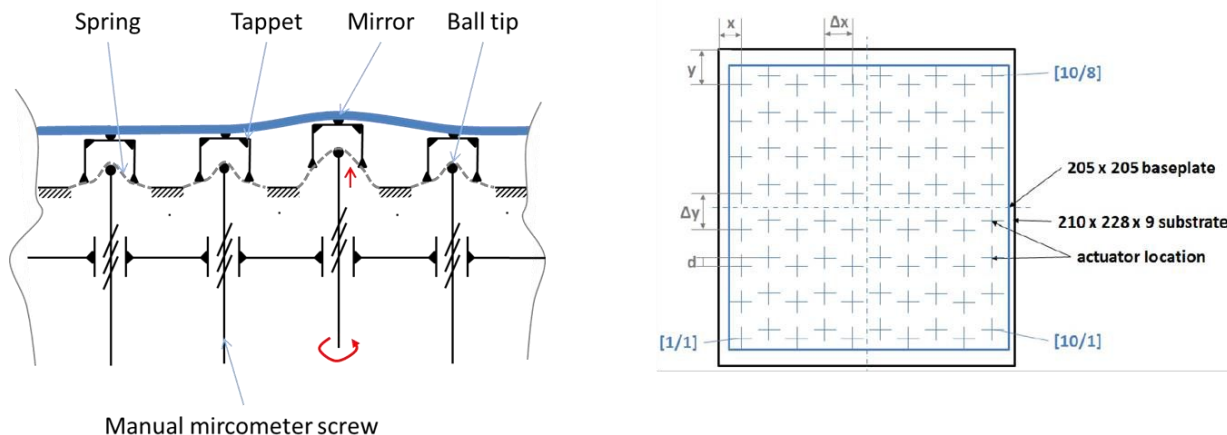


**Fig. 1.** Actuation mechanism of the active optics. Adapted from [1].

Figure 1(a) shows the actuation mechanism of the active optics. The mechanism was developed to achieve bi-direction actuation capability from a manual micrometer screw. At the same time, the mechanism should achieve superior stability after setting.

Therefore, we decided to use a flat spring to pre-load the screw. This ensures the good stability and enough stall force to push the screw in the housing. The screw without flat spring would have totter. The complete discussion of the flat spring design and is reported in [2], and here we just want to mention the actuator layout is a result of the pre-loading mechanism in that way that the actuators are spread to have a dense packing.

For the said applications, we designed, manufactured and tested an active support that capabilities will be characterized by the following sample mirror that is 228x210 mm<sup>2</sup> with 80 actuators as shown in Figure 2.

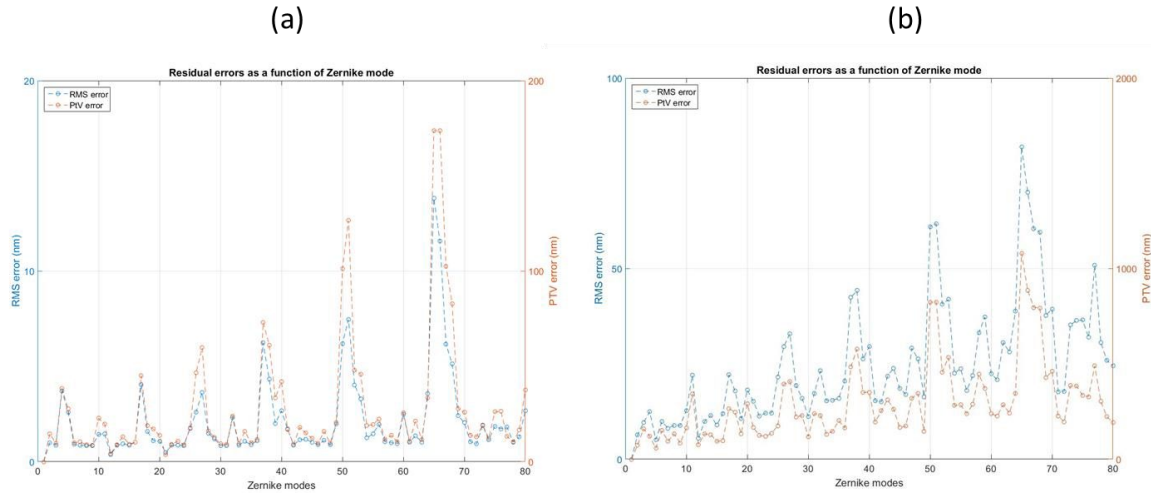


**Fig. 2.** 228x210 mm<sup>2</sup> sample mirror with 80 actuators.

Figure 1(b) shows the layout of an 80 degree-of-freedom active optics that is considered a hexagonal-type layout. From that layout we calculate the actuation capability of the device by the following routine:

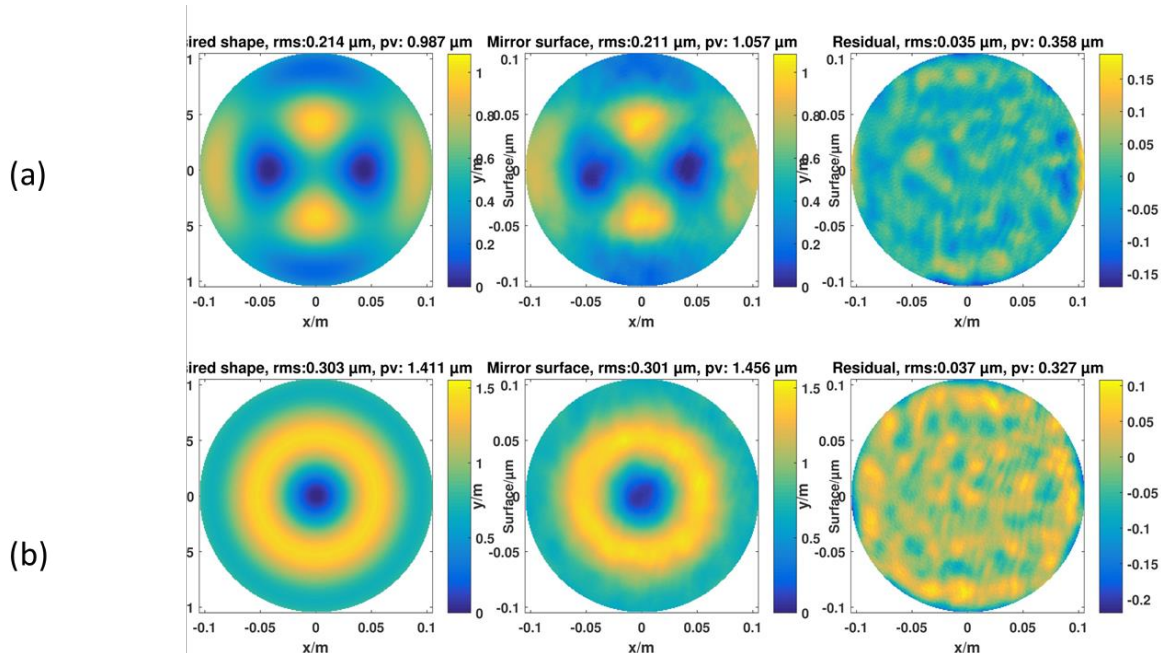
1. Definition of the desired shape in Zernike polynomial description to be compensated
2. Approximation of the actuator influence function by a Gaussian shape acting at each cross as shown in Fig. 2(b). Note, we assume that the influence of one actuator to the neighbored actuator is 50%. This is in accordance with our characterization measurements
3. Scaling of the actuator influence function to best fit the desired shape
4. Calculation of the difference surface between desired shape and best fit shape
5. Calculation of PtV and rms of the difference surface

Figure 3 gives the rms and PtV results for 80 Zernike modes that should be set with a PtV target deflection of 1.5  $\mu\text{m}$ . In (a) the ideal Gaussian shaped influence functions with 50% deflection on the neighbored actuators are applied and in (b) the Gaussian approximation of interferometrically measured influence functions are applied. It can be seen that in (a) the fitting results are excellent as beside four Zernikes all others may be set with an accuracy better 10 nm rms. Beside also the PtV values are remarkable low. In Fig. 2(b) it can be seen that the low order Zernike polynomials may be fit exceptionally as the low rms values indicate. On the other side, the PtV values of the difference surface are higher than expected. The comparison with Fig. 2(a) reveals that the same Zernike polynomials such as number 50/51, and 65/66 are only tolerably fit. Moreover, the approximated Gaussian actuator influence functions have also low values for other shapes such as 67/68. The ratio between rms and PtV values in Fig. 2(b) is worse than we expect from the theory.



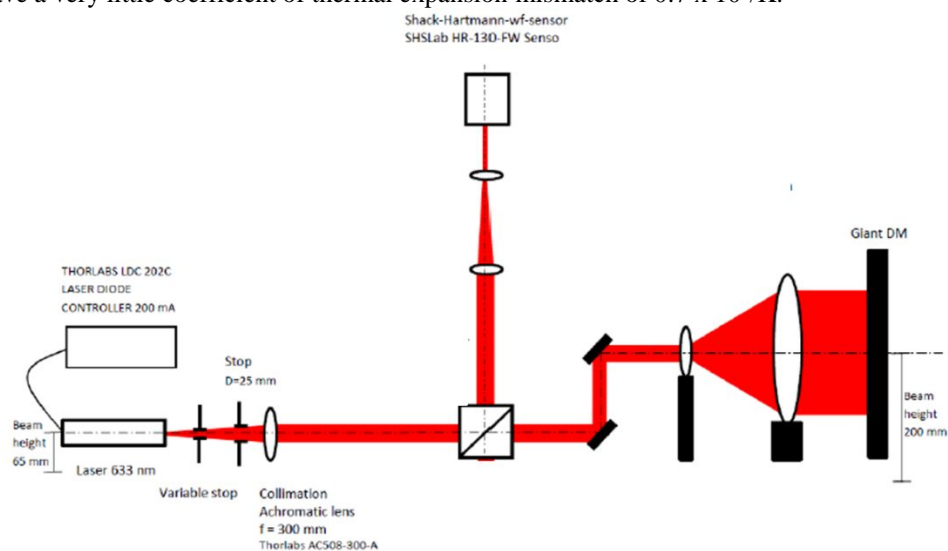
**Fig. 3.** Best fit rms and PtV results for 80 Zernike modes with a PtV target deflection of 1.5  $\mu\text{m}$ . In (a) the ideal Gaussian shaped influence functions with 50% deflection on the neighbored actuators are applied and in (b) the Gaussian approximation of interferometrically measured influence functions are applied.

Figure 4 shows two typical results of a worse fit. It can be seen that the residual surface is wavy and that the distance between the actuators condition the non-compensability of the Zernike polynomial. The waves have a smaller footprint than the actuator pitch. Generally, the actuator pitch gives the spatial correct ability of the active optics. However, this effect may just be observed with large amplitudes of the target shapes. Moreover, the sampling of the actuator influence function was with a manual setting of the deflections. Thus, the PtV of the actuator influence function varied a lot between the actuators. Moreover, we pushed some actuators and pulled others. The main reason for that was to maintain a relatively flat surface. However, the pre-loading on the actuators changed with the measurement resulting in different width of the actuator influence functions. Further, the actuator influence functions of the actuators on the rim may just likely fit with Gaussian shapes. This gives also the limit of this approximation. However, we wanted to show the capability of this manual device and better results might be achieved with motorized solutions. The device might be used to compensate for temperature-induced aberrations or manufacturing-induced aberrations. Both types are considered to be low-order aberrations.



**Fig. 4.** Typical result of residual difference surfaces between desired shape and fitted mirror surface. The residual is qualified by rms and PtV values.

Exceeding to the former publications on that device, we extended the long term stability measurements. The stability of the optical surface is measured interferometrically as reported in [2] over 90 days showing very stable and low wavefront errors (WFE) of  $WFE=(27\pm 2)$  nm rms. As a reminder, the absence of installation position depending effects was shown with a smaller sample in horizontal and vertical installation position. The temperature-induced deformations have been addressed with a Shack-Hartmann wavefront sensor based setup in a temperature controlled laboratory environment. The measurement set-up is shown in Figure 5. The beam of a HeNe-laser is collimated before it passes a beam splitter cube and two folding mirrors to lift the beam. Then a beam expander is used to expand the beam to  $\sim 200$  mm in diameter. After one week of temperature stabilization we started with the measurement of the reference surfaces. Then the temperature was decreased by 3K. After one week left for thermal stabilization, we made a large number of measurements and slowly increased the temperature to the starting value. However, the temperature-induced deformations of the mirror surface have been so small that it prevents determination from other temperature-induced changes of the measurement set-up. For a clear estimation of temperature-induced deformations, we would need to bring the mirror to a climate chamber and keep the measurement optics and sensor outside. On the other side, we expect only very little deformation as the baseplate/housing is made from INVAR and the mirror is manufactured from SQ1. Both materials have a very little coefficient of thermal expansion mismatch of  $0.7 \times 10^{-6}/K$ .



**Fig. 5.** Measurement set-up to detect temperature-induced mirror deformation in a temperature controlled laboratory environment.

## SUMMARY

We present the design of an active support for reflective optics. Then the aberration compensation performance is estimated by fitting of Zernike coefficients. Here, we draw a comparison between theoretical performance with a Gaussian shaped influence function and the performance with measured actuator influence functions. The purely theoretical values are excellent while the ones based on measurements have some loss in performance. However, the fitting capability is still high for low order aberrations. Then, we report on some extended long-term stability measurements showing no loss in stability over 90 days. Finally, the laboratory set-up to evaluate temperature-induced deformations is introduced. Although carefully working approach, we could not detect trustworthy values as the errors by the measurement set-up are in the same region or larger than the ones of the measurement device.

## REFERENCES

- [1] C. Reinlein ; A. Brady ; C. Damm ; M. Mohaupt ; A. Kamm ; N. Lange ; M. Goy; Long-term stable active mount for reflective optics. Proc. SPIE 9912, Advances in Optical and Mechanical Technologies for Telescopes and Instrumentation II, 99121N (July 22, 2016); doi:10.1117/12.2234729
- [2] C. Reinlein, C. Damm, N. Lange, A. Kamm, M. Mohaupt, A. Brady, M. Goy, N. Leonhard, R. Eberhardt, U. Zeitner, and A. Tünnermann, "Temporally-stable active precision mount for large optics," Opt. Express 24, 13527-13541 (2016).